Research article

Whole-eye electrical stimulation therapy preserves visual function and structure in P23H-1 rats

Adam M. Hanif [a, b, 1], Moon K. Kim [a, b, 1], Joel G. Thomas [c], Vincent T. Ciavatta [b], Micah Chrenek [a], John R. Hetling [c], Machelle T. Pardue [a, b, d, *]

[a] Department of Ophthalmology, Emory University School of Medicine, Atlanta, GA, USA
[b] Center for Visual and Neurocognitive Rehabilitation, Atlanta VA Medical Center, Decatur, GA, USA
[c] Bioengineering, University of Illinois at Chicago, Chicago, IL, USA
[d] Department of Biomedical Engineering, Georgia Institute of Technology, Atlanta, GA, USA

ARTICLE INFO

ABSTRACT

Low-level electrical stimulation to the eye has been shown to be neuroprotective against retinal degeneration in both human and animal subjects, using approaches such as subretinal implants and transcorneal electrical stimulation. In this study, we investigated the benefits of whole-eye electrical stimulation (WES) in a rodent model of retinitis pigmentosa. Transgenic rats with a P23H-1 rhodopsin mutation were treated with 30 min of low-level electrical stimulation (4 μA at 5 Hz; n = 10) or sham stimulation (Sham group; n = 15), twice per week, from 4 to 24 weeks of age. Retinal and visual functions were assessed every 4 weeks using electroretinography and optokinetic tracking, respectively. At the final time point, eyes were enucleated and processed for histology. Separate cohorts were stimulated once for 30 min, and retinal tissue harvested at 1 h and 24 h post-stimulation for real-time PCR detection of growth factors and inflammatory and apoptotic markers. At all time-points after treatment, WES-treated rat eyes exhibited significantly higher spatial frequency thresholds than untreated eyes. Inner retinal function, as measured by ERG oscillatory potentials (OPs), showed significantly improved OP amplitudes at 8 and 12 weeks post-WES compared to Sham eyes. Additionally, while photoreceptor segment and nuclei thicknesses in P23H-1 rats did not change between treatment groups, WES-treated eyes had significantly greater numbers of retinal ganglion cell nuclei than Sham eyes at 20 weeks post-WES. Gene expression levels of brain-derived neurotrophic factor (BDNF), caspase 3, fibroblast growth factor 2 (FGF2), and glutamine synthetase (GS) were significantly higher at 1 h, but not 24 h after WES treatment. Our findings suggest that WES has a beneficial effect on visual function in a rat model of retinal degeneration and that post-receptoral neurons may be particularly responsive to electrical stimulation therapy.

Published by Elsevier Ltd.

1. Introduction

The rehabilitative effects of electrical stimulation therapy (EST) in the eye have been observed since the 19th century (Dor, 1873). Offering benefit to muscle and neurons, the use of low levels of electrical current to improve visual function has manifested itself in a variety of approaches. In the retina, EST is administered in three major categories, based on the placement of the stimulating and reference electrodes: subretinal electrical stimulation (SES), transcorneal electrical stimulation (TES), and whole-eye electrical stimulation (WES). The nomenclature surrounding these different modes of EST has not been very consistent in the literature, thus, we provide the following descriptions of each type of stimulation. SES involves the use of implanted microphotodiode arrays, which deliver low level current to the inner retina in response to incident light (Pardue et al., 2005). The microphotodiode array consists of a microphotodiode array on the front surface that is referenced to the backside of the array (Chow et al., 2001; Pardue et al., 2005). Current density through this approach is estimated to be 100 μA (Pardue et al., 2005). TES has previously been used to describe any EST delivered to the corneal surface. However, in this manuscript,

* Corresponding author. Research Services (151 Oph), Atlanta VA Medical Center, 1670 Clairmont Road Decatur, GA 30033, USA.
E-mail address: Machelle.Pardue@bme.gatech.edu (M.T. Pardue).
[1] These authors contributed equally to this work.

we describe TES as delivery of stimulation to the eye when both the active and reference electrodes are both located on the ocular globe, such as with a bipolar contact lens electrode in human subjects (Fujikado et al., 2006; Inomata et al., 2007; Oono et al., 2011). In this way, electrical field and current are focused primarily in the anterior segment of the eye, rather than the inner retina as in SES (Pardue et al., 2014). Like TES, WES places an active electrode on the cornea, but the reference electrode is placed in the mouth or elsewhere on the head, permitting the current to become more uniformly distributed throughout the eye (Rahmani et al., 2013). This approach has often been referred to as TES in the literature and can be applied with a DTL electrode in animals and humans (Schatz et al., 2011, 2012) or contact lens in animal models (Willmann et al., 2011; Wrobel et al., 2011). Current magnitudes for TES and WES treatments range from 1.5 to 1000 μA (Pardue et al., 2014). Another EST approach is transorbital stimulation in which the electrodes are applied around the ocular orbit, but not directly on the eye in humans (Gall et al., 2011, 2015; Sabel et al., 2011; Schmidt et al., 2013).

While the methods of EST administration are diverse, their influence on the preservation of retinal structure and function is similar based on studies in animal models. In the RCS rat model of retinitis pigmentosa (RP), SES preserved outer nuclear layer (ONL) thickness (Pardue et al., 2005) and delayed inner retinal degeneration (Ciavatta et al., 2013). Similarly, TES-treated RCS retinas exhibited decreased apoptosis when isolated *ex vivo* (Schmid et al., 2009) and weekly sessions of 1-h TES therapy evoked preservation of ONL thickness (Morimoto et al., 2007). Light-induced retinal degeneration models also show preserved retinal structure after WES stimulation, such as reduced photoreceptor cell death and preserved outer segment length (Ni et al., 2009; Schatz et al., 2012). EST-induced protection is not limited to the outer retina. Sessions of TES every other day for two weeks preserved retinal ganglion cell (RGC) density in wild-type rats following ocular ischemia, a model of RGC death (Wang et al., 2011) or following optic nerve crush (Henrich-Noack et al., 2013).

Evidence that EST preserves retinal function includes reports that SES increased activity in the superior colliculus (DeMarco et al., 2007), and maintained electroretinogram (ERG) b-wave amplitudes (Pardue et al., 2005) in the RCS rat model of retinitis pigmentosa (RP). Regular TES and WES treatment preserve photoreceptor responsivity in rhodopsin mutation models of RP like the P347L rabbit (Morimoto et al., 2012) and P23H-1 rat (Rahmani et al., 2013), respectively. TES also preserves ERG b-waves and scotopic threshold response (STR) in RCS rats (Morimoto et al., 2007). Finally, TES modulates brain oscillations in the visual cortex after deafferentation that occurs after optic nerve crush in rats (Sergeeva et al., 2012, 2015).

Furthermore, up-regulation of neurotrophic factors in Muller cells is implicated in the mechanism of this protection (Zhou et al., 2012). Increased *in vivo* expression of fibroblast growth factor beta (FGF-2), insulin growth factor −1 (IGF-1), and brain derived neurotrophic factor (BDNF) have been observed after SES, TES and WES therapy, respectively (Ciavatta et al., 2009; Miyake et al., 2007; Ni et al., 2009). Furthermore, EST downregulates pro-inflammatory cytokines like tumor necrosis factor (TNF)-alpha, interleukin-1 beta (IL-1β) and pro-apoptotic gene Bax (Ni et al., 2009; Zhou et al., 2012).

While the physiological protection granted by retinal EST has been achieved through several methods, WES offers two unique advantages: 1) low-level electrical stimulation of the whole eye can be administered non-invasively (Rahmani et al., 2013), and 2) current delivery may be more uniformly distributed through the entire eye. In this study, we utilized WES in an attempt to observe the effects of uniform, non-invasive EST on visual and retinal function, retinal structure, and gene expression of growth factors and apoptotic factors in P23H-1 rats.

2. Methods

2.1. Animals

All animal procedures were approved by the Atlanta VA Institutional Animal Care and Use Committee and conform to the ARVO Statement for Use of Animals in Ophthalmic and Vision Research. Tg(P23H)1Lav line 1 (P23H-1) rats were kindly donated by Dr. Matthew LaVail (University of California, San Francisco) to generate an in-house breeding colony. Albino P23H-1 rats were bred with pigmented Long Evans rats (Charles River Laboratories, Raleigh, NC) to create the pigmented hemizygote P23H-1 rats that were used in these experiments. Rats were raised under 12:12 light:dark cycle with chow and water provided *ad libitum*.

2.2. WES procedure

P23H-1 rats were randomly divided into WES (n = 10) and Sham (n = 15) groups. Beginning at post-natal day 28 (P28), WES were anesthetized twice per week by an intraperitoneal injection of ketamine (60 mg/kg) and xylazine (7.5 mg/kg), and stimulated monocularly with controlled sine wave current (4 μA peak to peak at 5 Hz) for 30 min using a modified function generator, as previously described (Rahmani et al., 2013). Current was administered by placing one silver (Ag/AgCl) pellet electrode centrally on the cornea through a layer of eye lubricant (methylcellulose), referenced to a silver pellet electrode placed between the cheek and gums. This treatment regimen lasted for twenty weeks. Contralateral eyes were lubricated, but not stimulated. Following this same schedule, sham-treated animals were also anesthetized and received the same electrode placement, but were subjected to no electrical stimulation. Rats were placed on a heating pad during stimulation and treatment was applied at the same time of day for each cohort tested. After completion of the procedure, yohimbine (2.1 mg/kg) was administered to the rats to reverse the effects of xylazine and prevent corneal ulcers (Turner and Albassam, 2005).

2.3. Finite element modeling of WES

The approximate geometry of a rat head, including WES electrode locations, was built in SolidWorks (Dassault Systèmes SolidWorks Corporation, Waltham, MA), and imported into ANSYS for finite element analysis (FEA) of an electrostatic model. Electrical conductance of major tissue groups, including muscle, bone, skin and the major retinal layers, were included (Andreucetti et al., 1997). There have been procedural limitations in obtaining dielectric properties for all mammalian tissue types shortly after death and at low frequencies (Gabriel et al., 1996), and gradual alteration of these properties depending on animal age (Gabriel, 2005) and time post-mortem (Schmid et al., 2003; Surowiec et al., 1986) has been documented in the literature. Whereas this may lend an inherent uncertainty as to the absolute values of the current densities obtained from simulations, spatial distribution resulting from electrode positioning should remain unaffected by such factors. Fig. 1A shows a cutaway view of the meshed model with white circles indicating the location of the active and reference electrodes at the corneal surface and in the mouth, respectively. In simulation, a stimulating current of 10 μA was applied at the active electrode, with a potential of 0 V at the reference electrode. ANSYS solved Maxwell's equations for each node of the discretized model, giving voltages and current densities in the tissues that result from WES. Validation of this FEA model was accomplished by comparing
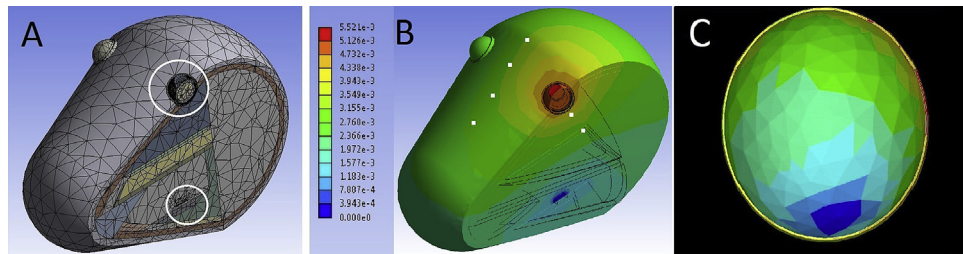
Fig. 1. Electrostatic model used for finite element analysis of the WES electrode configuration. A: Cross-sectional view, showing meshed model, white circles indicating electrode positions on cornea and in mouth. B: Contour plot of voltage; white squares mark measurement sites used in model validation (color scale $0-5.52e^{-3}$ V). C: Isolated photoreceptor layer from the electrostatic model plotting current density (color scale $0.396e^{-5}-0.142e^{-3}$ A/m^2).

simulated electrical potentials at several locations (small white squares in Fig. 1B) with measurements made on deceased rats (sacrificed immediately prior to measurements, n = 12) undergoing WES. Measurement locations were evenly spaced 1 cm apart, medially along the superior surface of the head and another two positioned at the inferior eyelid and 1 cm from the inferior eyelid of each eye, for a total of eight locations. The measurements were made with a platinum subdermal needle electrode, insulated except at the tip, which was inserted at each location to an approximate depth of 1 mm below the skin surface. WES of 10 μA at 1000 Hz was delivered via Ag/AgCl pellet electrodes at the eye and referenced to the mouth. Multiple measurements were taken from each insertion point in sequence. When normalized, the relative values between the eight locations were similar in the model simulations and the validation measurements.

2.4. Visual function measurements with optokinetic tracking (OKT)

Using a virtual system, we assessed visual function by analyzing spatial frequency thresholds evoked from optokinetic tracking behavior (OKT) (Prusky et al., 2004) (OptoMotry, Cerebral Mechanics, Inc., Lethbridge, Alberta, Canada). Testing was conducted at baseline prior to commencement of WES therapy, and repeated every four weeks. Briefly, rats were placed on a platform within an enclosed testing chamber and monitored remotely via a camera attached to the chamber ceiling. Computer monitors on each of the chamber's four walls projected moving spatial frequency gratings of different values. Reflexive optokinetic head-tracking in the same direction as the pattern of rotation was deemed a positive recognition. A staircase paradigm was used to find the highest spatial frequency threshold at which a tracking reflex could be elicited.

Both clockwise and counter-clockwise rotations were used to selectively attain thresholds for left and right eyes, respectively (Douglas et al., 2005). For analysis, spatial frequency thresholds measured from treated eyes were compared between WES and Sham groups. Additionally, the ratios of spatial frequencies for treated eyes over their contralateral, "opposite" eyes for each animal were averaged within each experimental group and compared.

2.5. Retinal function testing with electroretinography (ERG)

We assessed retinal function every four weeks starting from baseline, using ERG as previously detailed (Mocko et al., 2011). Briefly, rats were dark-adapted overnight and anesthetized [ketamine (60 mg/kg)/xylazine (7.5 mg/kg)] under dim red light. After anesthetizing the corneas (1% tetracaine) and dilating the pupils (1% tropicamide), rats were placed on a heating pad to maintain body temperature at 37 °C (ATC 1000; World Precision Instruments; Sarasota, FL). ERG stimuli consisted of a series of increasing flash stimuli presented by a Ganzfeld dome [Scotopic (-3.4 to 3.0 log cd s/m^2), Photopic (-0.8 to 2.0 log cd s/m^2); LKC

BigShot, Gaithersburg, MD]. Animals were light-adapted for 10 min prior to photopic ERG recordings. Electrical responses of the retina were recorded using a custom-made Dawson Trick Litzkow (DTL) fiber contacting the cornea through a layer of 1% methylcellulose (Dawson et al., 1979). Responses were referenced and grounded to 1 cm platinum needle electrodes inserted subcutaneously in the cheek and tail, respectively. We stored acquired responses on a commercial ERG system (UTAS 3000, LKC Technologies, Gaithersburg, MD), differentially amplified at 1–1500 Hz with a recording length of 250 ms and a digitization rate of 1.92 MHz. After testing, yohimbine (2.1 mg/kg) was administered to the rats to reverse effects of xylazine and prevent corneal ulcers (Turner and Albassam, 2005).

ERG data were analyzed offline. Amplitudes were manually measured for a- and b-waves, PII and oscillatory potentials (OP1-4), as previously described (Mocko et al., 2011). Dark-adapted a-waves, which originates in the rod photoreceptors (Hood and Birch, 1990), were measured from the baseline to the trough of the first negative wave. B-waves, which originate from the depolarizing bipolar cells (Stockton and Slaughter, 1989), were measured from the trough of the a-wave to the peak of the waveform, or when the a-wave was not present, from baseline to the peak of the waveform. OPs were digitally filtered using the ERG system software (75–500 Hz; EM Version 8.1.2, 2008; LKC), and manually measured from trough to peak. Scotopic PII was also filtered and measured, as previously described (Mocko et al., 2011). Baseline ERG testing was conducted before commencement of treatment, and then at 4 weeks, 8 weeks, 12 weeks, and 17 weeks during treatment.

2.6. Retinal structure analysis

After 20 weeks of stimulation therapy, rats were euthanized, and eyes were enucleated and marked superiorly for orientation. Eyes were immersion-fixed in 4% paraformaldehyde for 30 min, and then rinsed in 0.1 M phosphate buffer. After dissection to remove the lens and cornea, the posterior eye cup was dehydrated through a graded alcohol series and embedded in plastic resin (Embed 812/DER 736, Electron Microscopy Science, Inc, Hatfield, PA). Posterior hemispheres were sectioned in the superior to inferior plane (0.5 μm), using an ultramicrotome (Reichert Ultracut, Leica Inc., Buffalo Grove, IL) with a histo-diamond knife to bisect the optic disc. Retinal sections were then stained with 1% aqueous toluidine blue (Sigma; St. Louis MO), and imaged using a phase contrast microscope (Leica DMLB, Leica INc., Buffalo Grove, IL).

2.7. Measurement of retinal thickness and nuclei

Thicknesses of retinal layers (outer segments + inner segments, outer nuclear layer, outer plexiform layer, inner nuclear layer, inner plexiform layer, retinal ganglion cell layer) were measured for treated and non-treated eyes of WES (n = 4) and Sham (n = 3) rats
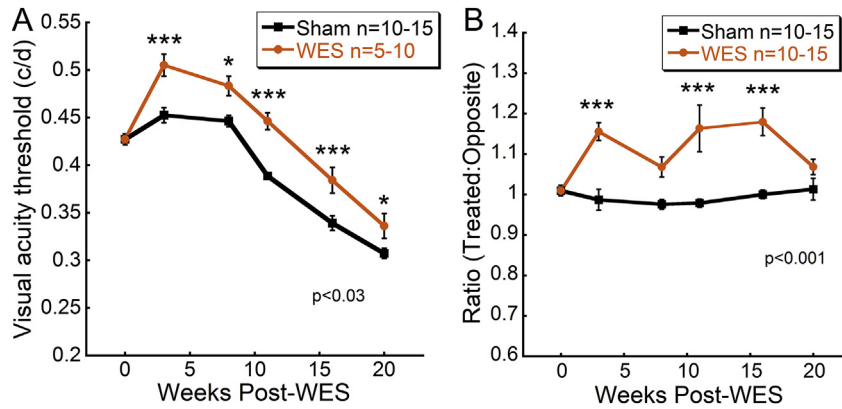
Fig. 2. WES preserves visual acuity in treated eyes. Visual acuity was preserved in WES-treated eyes. (A) Visual acuity in WES (n = 5–10) and Sham (n = 10–15) eyes was measured with OKT. At all time points after baseline, WES-treated eyes exhibited significantly greater preservation of spatial frequency thresholds (Two way repeated measures ANOVA, $F_{(5,129)} = 2.67$; p = 0.027). (B) Spatial frequency thresholds of each treated eye were divided by threshold values measured from their contralateral, untreated eyes. Eyes that received WES had significant increased visual acuity threshold ratios compared to contralateral eyes (Two way repeated measures ANOVA, $F_{(5,107)} = 7.744$; p < 0.001). Post-hoc comparisons: *p < 0.05, **p < 0.01, ***p < 0.001.

from 20× magnification images of retinal cross sections obtained via a phase contrast microscope (Leica DMLB, Leica Inc., Buffalo Grove, IL) using an image analysis program (Image-Pro Plus 5.0; Media Cybernetics, Warrendale, PA). Retinal regions spanning 2.5 mm superiorly and inferiorly from the optic nerve head were measured. Each 2.5 mm region was subdivided into five 0.5 mm sections and designated "F" or "S" 1–5 for inferior and superior, respectively. Thicknesses for each retinal layer were compared between Sham and WES groups at each location examined. Additionally, thicknesses across all locations examined for each retinal layer were averaged within experimental group and then compared.

RGC nuclei were quantified using an image analysis program (Image-Pro Plus 5.0; Media Cybernetics, Warrendale, PA). RGC counts were averaged in each of the ten regions in both WES (n = 5) and Sham (n = 9) eyes. Additionally, summed RGC counts of superior and inferior regions 1–4 were compared between experimental groups. All nuclei in the RGC layer were counted which included RGCs and any displaced amacrine cell nuclei.

2.8. Gene expression analysis of retinal tissue

At P28, a separate cohort of P23H-1 rats was randomly divided into WES or Sham groups. Each group received WES or sham treatment once for 30 min in the same manner described above. At either 1 h or 24 h after treatment, rats were sacrificed, and retinal tissue was obtained for real-time PCR (RT-PCR) analysis. RNA was isolated from retinal tissue and analyzed in real time for brain-derived neurotrophic factor (*Bdnf*), fibroblast growth factor 2 (*Fgf2*), insulin-like growth factor 1 (*Igf1*), ciliary nerve trophic factor (*Cntf*), glutamine synthetase (*Gs*), Caspase 3 (*Casp3*), BCL-2 associated X protein (*Bax*). Samples were run in triplicate, and the average Ct was calculated. With 18S as an internal standard, relative growth factor expression was calculated from the average PCR cycle thresholds using the $2^{-\Delta\Delta Ct}$ method (Rozen and Skaletsky, 2000). The expression ratio (treated eye/opposite eye) was computed to minimize between-animal variability in gene expression. Fold differences greater than 1.0 implied higher gene expression in the treated eye compared to the non-treated eye.

2.9. Statistical analysis

We performed one- and two-way repeated measures ANOVAs and Student's t-tests using commercial statistical analysis software

(SigmaStat 3.5; Systat Software; Chicago, IL). Reported p values are interaction effects unless otherwise indicated. We performed post-hoc multiple comparisons using the Holm-Sidak method. We set significance at p < 0.05 for all analyses and values are expressed as mean ± sem. The reported *n* is the total number of animals examined per group.

3. Results

3.1. WES generated a uniform stimulation across the entire retina

Fig. 1B is a contour plot of FEA simulation results, plotting voltages through the rat head during WES (range 0–5.52 mV). A goal in developing the WES approach (specifically, the electrode positions) was to achieve relatively uniform current density throughout the retina. Fig. 1C depicts the photoreceptor layer isolated from the rest of the model, plotting current density. Current density values across the retina had a mean of 92.76 μA/m^2 and standard deviation of 26.44 μA/m^2, yielding a coefficient of variation of 28.5%.

3.2. WES preserves visual function

At every testing point following the commencement of EST treatment, WES rats exhibited significantly greater spatial frequency thresholds than Sham rats (Fig. 2A; Two way repeated measures ANOVA, $F_{(5,129)} = 2.67$; p = 0.027). The spatial frequency threshold of WES-treated eyes increased by ~18% in the first 4 weeks and then maintained a steady ~11% higher threshold than the Sham eyes.

The average spatial frequency threshold ratios of treated vs. opposite eyes for each experimental group were also compared (Fig. 2B). These values for WES rats were significantly greater than Sham group animals at post-stimulation weeks 4, 12, and 17 (Two way repeated measures ANOVA, $F_{(5,107)} = 7.744$; p < 0.001), ranging from 7% to 18% greater than Sham from 4 to 17 weeks.

3.3. WES preserves inner retinal function

ERGs were conducted at baseline, and 4, 8, 12, and 17 week time points. No significant differences in amplitudes were found between experimental groups from a-wave, b-wave or isolated scotopic PII amplitudes at any time point or flash intensity (Supplemental Fig. 1). Additionally OP1-4 were measured and
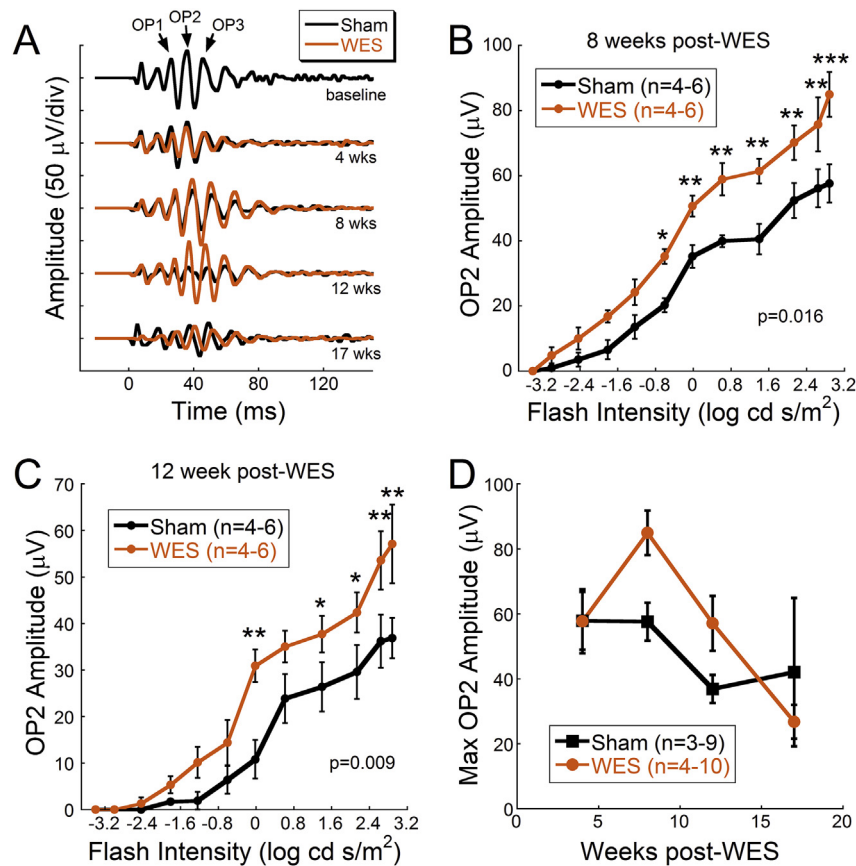
Fig. 3. WES preserves inner retinal function. (A) Representative dark-adapted OP responses to a bright flash (2.9 log cd s/m^2) across time in treated eyes for both WES and Sham groups. Differences in peak amplitudes between experimental groups were perceivable at 8 and 12 weeks post-WES. (B) OP2 amplitudes were significantly higher in WES-treated eyes in response to the brighter flash stimuli at 8 weeks post-WES (Two way repeated measures ANOVA, $F_{(11,107)} = 2.318$; $p = 0.016$) (C) Additionally, OP2 amplitudes remained significantly higher in WES-treated eyes compared to Sham for the brighter stimuli at 12 weeks post-WES (Two way repeated measures ANOVA, $F_{(11,155)} = 2.428$; $p = 0.009$) (D) Maximum OP2 amplitudes elicited from the brightest flash stimuli showed a trend for increased amplitudes in the WES-treated rats at 8 and 12 weeks compared to Sham, but no statistically significant differences were found. Post-hoc comparisons, $^*p < 0.05$, $^{**}p < 0.01$, $^{***}p < 0.001$.

compared. Representative OP waveforms at each time point across consecutive flash intensities revealed significant preservation of inner retinal function in WES-treated eyes at 8 and 12 week time points, though not sustained at 17 weeks (Fig. 3A). At 8 weeks post-WES, there was a significant interaction between treatment and flash intensity in OP2 amplitude between WES and Sham treated eyes (Fig. 3B; Two way repeated measures ANOVA, $F_{(11,107)} = 2.318$; $p = 0.016$). At 12 weeks post-WES, significant interactions between treatment and flash intensity were also identified (Fig. 3C, Two way repeated measures ANOVA, $F_{(11,155)} = 2.428$; $p = 0.009$). Examination of the maximum OP2 amplitudes elicited at the brightest flash across time showed trends for increased amplitudes at 8 and 12 weeks, but these did not reach significance (Fig. 3D; for OP1, OP3 and OP4 data, see Supplemental Fig. 2). We did not find any statistically significant differences in our photopic ERG b-wave data nor OP implicit times between WES and Sham eyes across the treatment period (data not shown).

3.4. WES preserves retinal ganglion cells

As shown in Fig. 4, the ONL was significantly thinned in the P23H-1 rats at 24 weeks of age, containing only 3—4 rows of photoreceptor nuclei compared to typical wild-type retinas which contain 10—12 rows (data not shown). Measurements of outer segment and inner photoreceptor segment thicknesses, ONL, inner nuclear layer and inner plexiform layer thickness confirmed no

differences between treatment groups (Supplemental Fig. 3). However, nuclei density in the ganglion cell layer (GCL) was visibly greater in WES rat retinas compared to Sham rats (Fig. 4A—B). Nuclei counts in the RGC layer were analyzed in retinal cross sections of WES and Sham group eyes. There was a significant interaction between treatment and region (Two way repeated measures ANOVA, $F_{(9,551)} = 2.638$; $p = 0.005$). Counts from two superior (Fig. 4C; S3, $p = 0.027$; S4, $p < 0.001$) and two inferior (Fig. 4C; F2, $p = 0.019$; F4, $p = 0.048$) 0.5 mm regions revealed significantly greater cell density in the RGC layer of WES rats ranging from 17 to 39%, although these difference were not observed for each region (see Fig. 4).

In addition, summed nuclei in the RGC layer from both inferior (Student's t-test, $p = 0.013$) and superior (Student's t-test; $p = 0.027$) regions were found to be significantly greater in WES rats than in Sham rats (Fig. 4D). This was a 16 and 12% increase, respectively, in cellular nuclei density in the RGC layer of WES retinas compared to Sham. Finally, total cellular density in the RGC layer from all regions yielded similar results with a 14% increase in WES retinas compared to Sham (Student's t-test; $p = 0.005$).

3.5. WES upregulates specific growth factors

Relative expression of *Bdnf*, *Fgf2*, *Igf1*, *Cntf*, *Gs*, *Casp3*, and *Bax*, was analyzed in WES or Sham treated eyes at 1 and 24 h after a 30 min WES session. One hour after a 30 min WES therapy session,
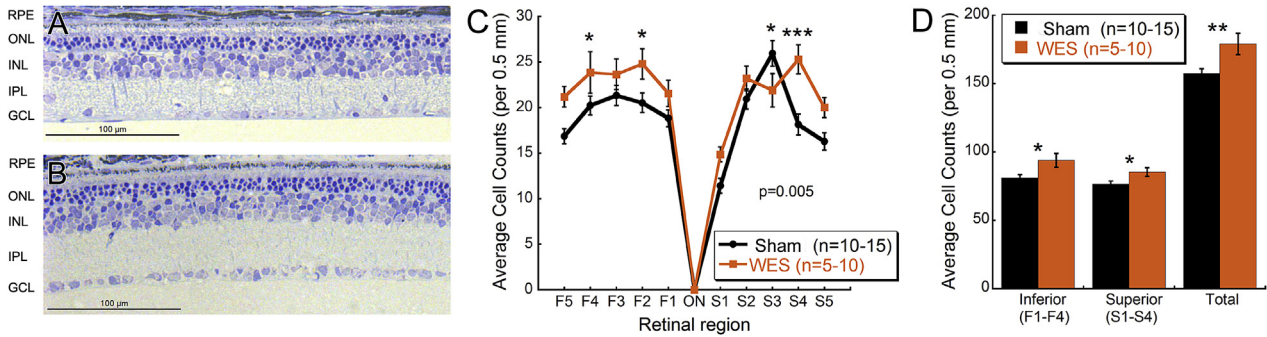
Fig. 4. WES preserves RGCs. Representative images of retinal cross sections from Sham (A) and WES (B) treated eyes. Cellular density in the RGC layer is visibly more robust in WES treated eyes, indicating that electrical stimulation of the whole eye preserved retinal morphology in the P23H-1 model. (C) WES-treated eyes yielded greater RGC counts than Sham treated eyes (Two way repeated measures ANOVA, $F_{(9,551)} = 2.638$; $p = 0.005$) (D) Sums of inferior (Student's t-test, $p = 0.013$) and superior (Student's t-test; $p = 0.027$) regions 1—4 between groups also revealed significantly greater nuclei in the RGC layer of WES treated eyes. Sums of all regions (Total) showed more RGC layer cells in the WES-treated eyes (Student's t-test; $p = 0.005$). Post-hoc comparisons: $^*p < 0.05$, $^{**}p < 0.01$, $^{***}p < 0.001$.
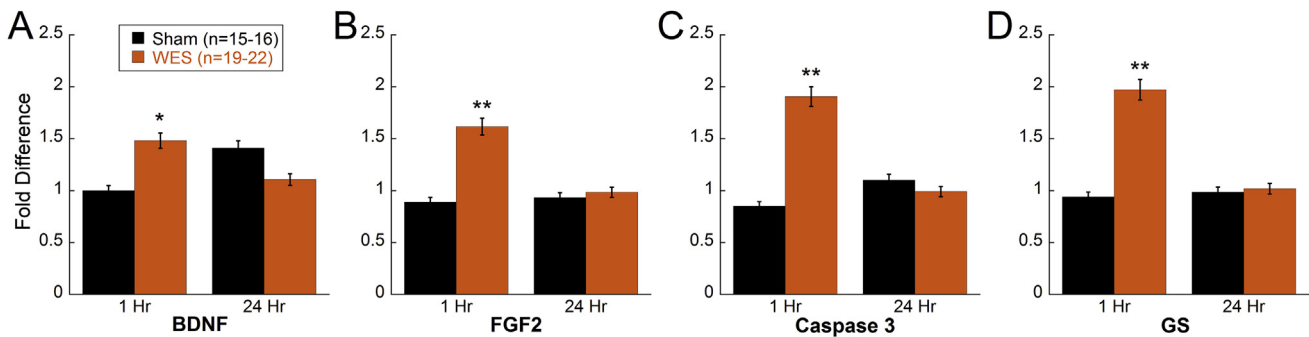

Fig. 5. WES upregulates specific growth factors and apoptotic markers. RT-PCR analysis revealed elevated expression of (A) *Bdnf* (Two way ANOVA, $F_{(1,71)} = 7.064$; $p = 0.01$), (B) *Fgf2* (Two way ANOVA, $F_{(1,65)} = 4.956$; $p = 0.03$), (C) *Casp3* (Two way ANOVA, $F_{(1,69)} = 5.223$; $p = 0.026$), and (D) *Gs* (Two way ANOVA, $F_{(1,66)} = 5.197$; $p = 0.03$) in P23H-1 rats (aged 4 weeks) subjected to one 30-min session of WES and sacrificed 1 h after treatment compared to Sham eyes. No significant differences in gene expression were detected in retinas harvested 24 h after WES therapy. Asterisks indicate post-hoc comparisons: $^*p < 0.05$, $^{**}p < 0.01$.

significantly greater expression of *Bdnf* (Two way ANOVA, $F_{(1,71)} = 7.064$; $p = 0.01$) and *Fgf2* (Two way ANOVA, $F_{(1,65)} = 4.956$; $p = 0.03$) were measured in the WES-treated retinas (Fig. 5A and B). In addition, *Casp3* (Two way ANOVA, $F_{(1,69)} = 5.223$; $p = 0.026$) and *Gs* (Two way ANOVA, $F_{(1,66)} = 5.197$; $p = 0.03$) levels were also significantly higher than Sham treated eyes at 1 h (Fig. 5C and D). However, *Igf1*, *Cntf*, and *Bax* showed no differences in expression at 1 h post-stimulation (Supplemental Fig. 4). At 24 h after WES stimulation, the gene expression levels were not different for any of the genes tested. *Bax* expression was reduced in all WES treated eyes compared to control eyes (main effect of treatment Two-way ANOVA $F_{(1, 48)} = 7.58$, $p < 0.01$; Supplemental Fig. 4).

4. Discussion

In this study, we utilized a non-invasive approach to delivering low levels of electrical stimulation to the whole eye in a rodent model of RP. WES-treated rats exhibited significantly greater preservation of visual acuity for the 20 week duration of stimulation and greater inner retinal function. Additionally, after twenty weeks of a twice-per-week WES treatment schedule, RGC counts in WES-treated eyes of P23H-1 rats were significantly higher than unstimulated rats of the same strain. These data, in addition to significantly greater fold differences for protective growth factors in eyes subjected to our treatment paradigm, indicate that routine WES therapy has the potential to offer selective, prolonged preservation of structure and function to the degenerating retina.

WES therapy offered significant preservation of nuclei in the RGC layer of the P23H-1 rat, a rodent model of RP. A spectrum of inheritable degenerative retina disorders, retinitis pigmentosa is a prominent and incurable cause of human blindness characterized by a progressive loss of rod photoreceptors, followed by cones (Merin and Auerbach, 1976; Wenzel et al., 2005; Yu et al., 2004). While several genes have been implicated to cause RP, approximately 30—40% can be attributed to genetic rhodopsin defects such as the P23H mutation (Ferrari et al., 2011). The P23H defect is implicated in a high number of North American RP cases due to an autosomal dominant mutation in the rhodopsin gene which results in photoreceptor death (Berson et al., 1991). The P23H rat model is widely used to model autosomal dominant RP and the P23H-1 rat has been shown to have progressive rod-cone dysfunction and outer retina thinning (Orhan et al., 2015). In these experiments, we used the P23H-1 rat to extend our previous research with this model (Rahmani et al., 2013).

However RP-related retinal degeneration is not limited to the outer nuclear layer. In humans, alteration of all layers of the retina has been observed with time, including RGC loss (Fariss et al., 2000; Milam et al., 1998; Villegas-Perez et al., 1996). Similarly, electrophysiological and histological observations in the P23H-1 rat have implicated significant RGC loss by 6 months of age as part of the retinal complications accompanying this model (Garcia-Ayuso et al., 2010, 2013; Orhan et al., 2015). Our measurements of retinal OS + IS and ONL thicknesses in WES and Sham treated eyes (Supplemental Fig. 3) indicated that the electrical stimulation therapy did not have a significant effect in preserving photoreceptor density in the P23H-1 rat nor photoreceptor function as

measured by the ERG a-wave (Supplemental Fig. 1). However, reports of RGC death in the P23H phenotype (Fransen et al., 2015; Garcia-Ayuso et al., 2010, 2015; Sekirnjak et al., 2011) and involvement of RGCs in response to electrical stimulation (Foik et al., 2015; Potts and Inoue, 1969) compelled us to monitor RGC loss which led to a finding of significant protection by approximately 6 months of age due to WES therapy. Our data suggest that post-receptoral neurons were particularly responsive to the electrical stimulation, exhibiting significant preservation for up to twenty weeks of treatment.

WES treatment preserved ERG OP amplitudes between 8 and 12 weeks post-WES. OPs are thought to reflect the activity of the amacrine cells in the inner retina. A limitation of the current study is suboptimal bandpass filtering setting for the rat retina that may have missed some lower frequency components of the OPs (Zhang et al., 2007). However, the current filter settings did provide clear analysis of the higher frequency components without potential interference from the a- or b-waves. While we did not find measureable differences in inner retinal thickness between the WES and Sham eyes (Supplemental Fig. 3), we did find increased cell counts in the RGC layer of WES eyes. Since our RGC counts included all cells within the RGC layer, including any displaced amacrine cells, our functional and structural results may suggest that WES eyes have preserved displaced amacrine cells. ERG OP amplitudes significantly declined between 12 and 17 weeks post-WES (16–21 weeks of age), an age at which the ONL thickness of the P23H-1 rats is reduced to ~25% of WT (Orhan et al., 2015). Thus, the absence of sustained benefit from WES may be due to the progressive nature of the degeneration that is affecting outer and inner retinal layers by this stage of disease. These results may indicate that WES is most beneficial in early to mid-disease before major loss of retinal neurons occurs. With the finding of significantly preserved RGCs, it is not surprising that the full-field ERG would not reveal significant differences for the a- and b-wave as these waves originates from the photoreceptor (Penn and Hagins, 1969; Robson and Frishman, 1998), and bipolar cells (Bush and Sieving, 1996; Hood and Birch, 1996; Robson and Frishman, 1995; Sieving et al., 1994), respectively. Future studies are needed to specifically probe RGC function using pattern ERG, visually evoked potentials or the photopic negative response to further delineate the source of neuro-preservation with WES.

RGC preservation is likely implicated in the improved visual function observed in the WES-treated retinas. Our functional testing scheme included the implementation of OKT to assess preservation of visual acuity in the P23H-1 rat due to WES therapy. Interestingly, WES-treated rats exhibited significantly higher visual acuity in their treated eyes than did Sham rats. This improvement in visual function could be due in part to the observed preservation of cellular density in the RGC layer of stimulated eyes. OKT testing of glaucomatous DBA/2J mice, a preclinical mouse model of spontaneous glaucoma, revealed a marked decrease in visual acuity in parallel with onset of glaucoma, a condition characterized by progressive RGC death (Burroughs et al., 2011). It is likely that preservation of RGC's in the P23H-1 model is similarly related to corresponding performance on visual acuity tests. Furthermore, untreated eyes yielded significantly lower visual acuity thresholds than their contralateral WES-treated eyes, indicating a selective preservation of function due to stimulation.

Our findings suggest possible mechanisms by which WES therapy may orchestrate this observed protection. RT-PCR revealed significant elevation of *Bdnf* and *Fgf2* expression in WES-treated retinas after only 1 h of stimulation. Implicated in the preservation of retinal cells undergoing degeneration due to toxic light (LaVail et al., 1992) and ischemic injury (Unoki and LaVail, 1994), *Bdnf* has been previously documented to be expressed in Muller

cells given WES therapy *in vivo* (Ni et al., 2009), as well as cultured Muller cells exposed to biphasic pulses (10 μA, 1 ms pulse duration, 20 Hz) (Sato et al., 2008a). Additionally, elevated *Fgf2* presence has been detected in retinas given SES implants (Ciavatta et al., 2013), as well as cultured Muller cells treated with biphasic electrical pulses (Sato et al., 2008c). Our findings not only reinforce what is known about *Bdnf* expression in the WES-treated retina, but also contribute *Fgf2* for the first time as a mediator of retinal preservation to the mosaic of observed growth factors upregulated during WES therapy.

WES therapy also seems to increase *Gs* expression, which may provide higher rates of glutamate turnover and decrease susceptibility to glutamate excitotoxicity which has been implicated in models of retinal degeneration including the rd1 mouse, RCS rat, streptozotocin (STZ) induced diabetic retinopathy, and anterior optic neuropathy (Allen et al., 2014; Delyfer et al., 2005; Liu et al., 2013; Shaked et al., 2002; Yu et al., 2009). While dysregulation of glutamate has been connected with the pathogenesis of retinal degeneration, GS has also been found to mediate the onset of and recovery from retinal injury (Barnett et al., 2000; Gorovits et al., 1997). In a TES therapy paradigm, Wang et al. reported significant preservation of RGCs, ERG b-wave and GS levels after ischemic injury in rats (Wang et al., 2011). It is likely that the observed elevation of *Gs* presence may in part be due to our WES treatment paradigm, and precluded considerable glutamate excitotoxicity implicated in models of RP similar to the P23H-1 rat.

Our data also reflect significant up regulation of *Casp3*. While frequently associated with the execution of cell death (Stroh and Schulze-Osthoff, 1998; Utz and Anderson, 2000), Caspase 3 also plays a role in cell survival under conditions of mild stress (Yang et al., 2004). We hypothesize that the mild stress of prolonged electrical stimulation may be sufficient for the retina to recruit caspase 3 in quantities to cleave RasGAP, activate Akt, and improve the longevity of retinal cells undergoing the degeneration of the P23H-1 phenotype (Khalil et al., 2012, 2014; Yang et al., 2004).

These gene expression results show that gene expression changes occur quickly, by 1hr post-WES and are back to normal by 24 h post-WES. These results suggest that daily WES stimulation may produce larger protective effects in sustaining gene expression changes and therefore, possibly further improve functional and structural outcome, than if stimulation occurs twice per week, as done here. Future experiments will determine if repeated daily WES will produce sustained increased in expression of growth factors. Past experiments to test dose response of SES was not able to show a dose-dependent increase in FGF2 gene expressions (Ciavatta et al., 2013). However, future experiments are needed to determine if larger doses of WES would produce increased gene expression or if gene expression would be different if measured at a different stage of degeneration, before the majority of photoreceptors have been lost.

These results extend the findings from the Rahmani et al. study which also tested the protective effects of WES on P23H-1 rats, as well as extending our previous work with SES to a non-invasive approach (Rahmani et al., 2013; Pardue et al., 2005). In choosing the WES current level for the current study, we consider the fact that larger protective effects of retinal function had been found for SES than WES. Thus, for this study we chose a 4 μA current, nearly 3 times larger than the 1.5 μA used in the Rahami et al. study, but much lower than the current used for SES and TES which ranges from 100 to 900 μA (Pardue et al., 2014). Thus, our inability to replicate the preserved b-wave and rod sensitivity found in Rahami et al. may be due to the higher current levels. While SES current preserved photoreceptor structure in the RCS rat (Pardue et al., 2005), WES at 1.5 μA (Rahmani et al., 2013) or 4 μA (current study) did not preserve the outer retina in the P23H-1 rat. Further

research is needed to determine if EST is equally effective for all types of photoreceptor degeneration.

In addition to characterizing this mode of electrical stimulation in the P23H-1 rat, our findings may support and help explain the findings regarding the effects of such therapy in the human eye. RP patients subjected to TES experienced preservation of visual field area and ERG b-wave amplitude (Schatz et al., 2011). Up-regulation of *Bdnf*, *Casp3*, *Gs* and *Fgf2* reveal possible mechanisms of this effect in the P23H-1 rat model, but potentially also in humans. For instance, clinical studies showing the benefit of TES studies on RGC damage may have similar mechanisms. After 30 min of TES, patients with nonarteritic ischemic optic neuropathy or traumatic optic neuropathy showed preservation of visual acuity and retinal function (Fujikado et al., 2006) and patients with optic nerve damage had larger visual fields after 20—40 min of transorbital alternating current stimulation (Gall et al., 2011). Future studies are needed to determine if RGC models have similar increases in growth factor expression. Interestingly, we did not witness changes in molecules like *Cntf*, *Igf-1*, and *Bax*, which have been noted in previous investigations of EST, though not necessarily WES (Ni et al., 2009; Sato et al., 2008b).

5. Conclusions

In summary, our findings indicated that electrical stimulation to the whole eye offers preservation of visual acuity and cellular density in the RGC layer, mediated by up-regulation of *Bdnf*, *Fgf2*, *Gs*, and *Casp3*. Future experiments would aim to identify optimal simulation parameters that might yield greater preservation of electrophysiological response in addition to greater visual acuity and RGC density, and significant changes in a fuller spectrum of protective mediators. Low-level electrical stimulation of the whole eye is a potential therapy by which retinal degeneration patients may protect and maintain vision through a safe, non-invasive approach.

Acknowledgements:

Appendix A. Supplementary data

Supplementary data related to this article can be found at http://dx.doi.org/10.1016/j.exer.2016.06.010.

References

Allen, R.S., Sayeed, I., Cale, H.A., Morrison, K.C., Boatright, J.H., Pardue, M.T., Stein, D.G., 2014. Severity of middle cerebral artery occlusion determines retinal deficits in rats. Exp. Neurol. 254, 206—215.

Andreucetti, D., Rossi, R., Petrucci, C., 1997. An Internet Resource for the Calculation of the Dielectric Properties of Body Tissues in the Frequency Range 10 Hz — 100 GHz. IFAC-CNR, Florence, Italy. http://niremf.ifac.cnr.it/tissprop/.

Barnett, N.L., Pow, D.V., Robinson, S.R., 2000. Inhibition of Muller cell glutamine synthetase rapidly impairs the retinal response to light. Glia 30, 64—73.

Berson, E.L., Rosner, B., Sandberg, M.A., Dryja, T.P., 1991. Ocular findings in patients with autosomal dominant retinitis pigmentosa and a rhodopsin gene defect (Pro-23-His). Arch. Ophthalmol. 109, 92—101.

Burroughs, S.L., Kaja, S., Koulen, P., 2011. Quantification of deficits in spatial visual function of mouse models for glaucoma. Investig. Ophthalmol. Vis. Sci. 52, 3654—3659.

Bush, R.A., Sieving, P.A., 1996. Inner retinal contributions to the primate photopic fast flicker electroretinogram. J. Opt. Soc. Am. A Opt. Image Sci. Vis. 13, 557—565.

Chow, A.Y., Pardue, M.T., Chow, V.Y., Peyman, G.A., Liang, C., Perlman, J.I., Peachey, N.S., 2001. Implantation of silicon chip microphotodiode arrays into the cat subretinal space. IEEE Trans. Neural Syst. Rehabil. Eng. 9, 86—95.

Ciavatta, V.T., Kim, M., Wong, P., Nickerson, J.M., Shuler Jr., R.K., McLean, G.Y., Pardue, M.T., 2009. Retinal expression of Fgf2 in RCS rats with subretinal microphotodiode array. Investig. Ophthalmol. Vis. Sci. 50, 4523—4530.

Ciavatta, V.T., Mocko, J.A., Kim, M.K., Pardue, M.T., 2013. Subretinal electrical stimulation preserves inner retinal function in RCS rat retina. Mol. Vis. 19, 995—1005.

Dawson, W.W., Trick, G.L., Litzkow, C.A., 1979. Improved electrode for electroretinography. Investig. Ophthalmol. Vis. Sci. 18, 988—991.

Delyfer, M.N., Forster, V., Neveux, N., Picaud, S., Leveillard, T., Sahel, J.A., 2005. Evidence for glutamate-mediated excitotoxic mechanisms during photoreceptor degeneration in the rd1 mouse retina. Mol. Vis. 11, 688—696.

DeMarco Jr., P.J., Yarbrough, G.L., Yee, C.W., McLean, G.Y., Sagdullaev, B.T., Ball, S.L., McCall, M.A., 2007. Stimulation via a subretinally placed prosthetic elicits central activity and induces a trophic effect on visual responses. Investig. Ophthalmol. Vis. Sci. 48, 916—926.

Dor, H., 1873. Beiträge zur Electrotherapie der Augenkrankheiten. Albr. Graefes Arch. Ophthalmol. 19, 316—352.

Douglas, R.M., Alam, N.M., Silver, B.D., McGill, T.J., Tschetter, W.W., Prusky, G.T., 2005. Independent visual threshold measurements in the two eyes of freely moving rats and mice using a virtual-reality optokinetic system. Vis. Neurosci. 22, 677—684.

Fariss, R.N., Li, Z.Y., Milam, A.H., 2000. Abnormalities in rod photoreceptors, amacrine cells, and horizontal cells in human retinas with retinitis pigmentosa. Am. J. Ophthalmol. 129, 215—223.

Ferrari, S., Di Iorio, E., Barbaro, V., Ponzin, D., Sorrentino, F.S., Parmeggiani, F., 2011. Retinitis pigmentosa: genes and disease mechanisms. Curr. Genomics 12, 238—249.

Foik, A.T., Kublik, E., Sergeeva, E.G., Tatlisumak, T., Rossini, P.M., Sabel, B.A., Waleszczyk, W.J., 2015. Retinal origin of electrically evoked potentials in response to transcorneal alternating current stimulation in the rat. Investig. Ophthalmol. Vis. Sci. 56, 1711—1718.

Fransen, J.W., Pangeni, G., Pyle, I.S., McCall, M.A., 2015. Functional changes in Tg P23H-1 retinal responses: differences between ON and OFF pathway transmission to the superior colliculus. J. Neurophysiol. 114, 2368—2375.

Fujikado, T., Morimoto, T., Matsushita, K., Shimojo, H., Okawa, Y., Tano, Y., 2006. Effect of transcorneal electrical stimulation in patients with nonarteritic ischemic optic neuropathy or traumatic optic neuropathy. Jpn. J. Ophthalmol. 50, 266—273.

Gabriel, C., 2005. Dielectric properties of biological tissue: variation with age. Bioelectromagnetics (Suppl. 7), S12—S18.

Gabriel, S., Lau, R.W., Gabriel, C., 1996. The dielectric properties of biological tissues: II. Measurements in the frequency range 10 Hz to 20 GHz. Phys. Med. Biol. 41, 2251—2269.

Gall, C., Sgorzaly, S., Schmidt, S., Brandt, S., Fedorov, A., Sabel, B.A., 2011. Noninvasive transorbital alternating current stimulation improves subjective visual functioning and vision-related quality of life in optic neuropathy. Brain Stimul. 4, 175—188.

Gall, C., Silvennoinen, K., Granata, G., de Rossi, F., Vecchio, F., Brosel, D., Bola, M., Sailer, M., Waleszczyk, W.J., Rossini, P.M., Tatlisumak, T., Sabel, B.A., 2015. Non-invasive electric current stimulation for restoration of vision after unilateral occipital stroke. Contemp. Clin. Trials 43, 231—236.

Garcia-Ayuso, D., Di Pierdomenico, J., Esquiva, G., Nadal-Nicolas, F.M., Pinilla, I., Cuenca, N., Vidal-Sanz, M., Agudo-Barriuso, M., Villegas-Perez, M.P., 2015. Inherited photoreceptor degeneration causes the death of melanopsin-positive retinal ganglion cells and increases their coexpression of Brn3a. Investig. Ophthalmol. Vis. Sci. 56, 4592—4604.

Garcia-Ayuso, D., Ortin-Martinez, A., Jimenez-Lopez, M., Galindo-Romero, C., Cuenca, N., Pinilla, I., Vidal-Sanz, M., Agudo-Barriuso, M., Villegas-Perez, M.P., 2013. Changes in the photoreceptor mosaic of P23H-1 rats during retinal degeneration: implications for rod-cone dependent survival. Investig. Ophthalmol. Vis. Sci. 54, 5888—5900.

Garcia-Ayuso, D., Salinas-Navarro, M., Agudo, M., Cuenca, N., Pinilla, I., Vidal-Sanz, M., Villegas-Perez, M.P., 2010. Retinal ganglion cell numbers and delayed retinal ganglion cell death in the P23H rat retina. Exp. Eye Res. 91, 800—810.

Gorovits, R., Avidan, N., Avisar, N., Shaked, I., Vardimon, L., 1997. Glutamine synthetase protects against neuronal degeneration in injured retinal tissue. Proc. Natl. Acad. Sci. U. S. A. 94, 7024—7029.

Henrich-Noack, P., Voigt, N., Prilloff, S., Fedorov, A., Sabel, B.A., 2013. Transcorneal electrical stimulation alters morphology and survival of retinal ganglion cells after optic nerve damage. Neurosci. Lett. 543, 1—6.

Hood, D.C., Birch, D.G., 1990. A quantitative measure of the electrical activity of human rod photoreceptors using electroretinography. Vis. Neurosci. 5, 379—387.

Hood, D.C., Birch, D.G., 1996. Beta wave of the scotopic (rod) electroretinogram as a measure of the activity of human on-bipolar cells. J. Opt. Soc. Am. A Opt. Image Sci. Vis. 13, 623—633.

Inomata, K., Shinoda, K., Ohde, H., Tsunoda, K., Hanazono, G., Kimura, I., Yuzawa, M., Tsubota, K., Miyake, Y., 2007. Transcorneal electrical stimulation of retina to treat longstanding retinal artery occlusion. Graefes Arch. Clin. Exp. Ophthalmol.

245, 1773–1780.

Khalil, H., Bertrand, M.J., Vandenabeele, P., Widmann, C., 2014. Caspase-3 and RasGAP: a stress-sensing survival/demise switch. Trends Cell Biol. 24, 83–89.

Khalil, H., Peltzer, N., Walicki, J., Yang, J.Y., Dubuis, G., Gardiol, N., Held, W., Bigliardi, P., Marsland, B., Liaudet, L., Widmann, C., 2012. Caspase-3 protects stressed organs against cell death. Mol. Cell Biol. 32, 4523–4533.

LaVail, M.M., Unoki, K., Yasumura, D., Matthes, M.T., Yancopoulos, G.D., Steinberg, R.H., 1992. Multiple growth factors, cytokines, and neurotrophins rescue photoreceptors from the damaging effects of constant light. Proc. Natl. Acad. Sci. U. S. A. 89, 11249–11253.

Liu, K., Wang, Y., Yin, Z., Weng, C., Zeng, Y., 2013. Changes in glutamate homeostasis cause retinal degeneration in royal college of surgeons rats. Int. J. Mol. Med. 31, 1075–1080.

Merin, S., Auerbach, E., 1976. Retinitis pigmentosa. Surv. Ophthalmol. 20, 303–346.

Milam, A.H., Li, Z.Y., Fariss, R.N., 1998. Histopathology of the human retina in retinitis pigmentosa. Prog. Retin Eye Res. 17, 175–205.

Miyake, K., Yoshida, M., Inoue, Y., Hata, Y., 2007. Neuroprotective effect of transcorneal electrical stimulation on the acute phase of optic nerve injury. Investig. Ophthalmol. Vis. Sci. 48, 2356–2361.

Mocko, J.A., Kim, M., Faulkner, A.E., Cao, Y., Ciavatta, V.T., Pardue, M.T., 2011. Effects of subretinal electrical stimulation in mer-KO mice. Investig. Ophthalmol. Vis. Sci. 52, 4223–4230.

Morimoto, T., Fujikado, T., Choi, J.S., Kanda, H., Miyoshi, T., Fukuda, Y., Tano, Y., 2007. Transcorneal electrical stimulation promotes the survival of photoreceptors and preserves retinal function in royal college of surgeons rats. Investig. Ophthalmol. Vis. Sci. 48, 4725–4732.

Morimoto, T., Kanda, H., Kondo, M., Terasaki, H., Nishida, K., Fujikado, T., 2012. Transcorneal electrical stimulation promotes survival of photoreceptors and improves retinal function in rhodopsin P347L transgenic rabbits. Investig. Ophthalmol. Vis. Sci. 53, 4254–4261.

Ni, Y.Q., Gan, D.K., Xu, H.D., Xu, G.Z., Da, C.D., 2009. Neuroprotective effect of transcorneal electrical stimulation on light-induced photoreceptor degeneration. Exp. Neurol. 219, 439–452.

Oono, S., Kurimoto, T., Kashimoto, R., Tagami, Y., Okamoto, N., Mimura, O., 2011. Transcorneal electrical stimulation improves visual function in eyes with branch retinal artery occlusion. Clin. Ophthalmol. 5, 397–402.

Orhan, E., Dalkara, D., Neuille, M., Lechauve, C., Michiels, C., Picaud, S., Leveillard, T., Sahel, J.A., Naash, M.I., Lavail, M.M., Zeitz, C., Audo, I., 2015. Genotypic and phenotypic characterization of P23H line 1 rat model. PLoS One 10, e0127319.

Pardue, M.T., Ciavatta, V.T., Hetling, J.R., 2014. Neuroprotective effects of low level electrical stimulation therapy on retinal degeneration. Adv. Exp. Med. Biol. 801, 845–851.

Pardue, M.T., Phillips, M.J., Yin, H., Sippy, B.D., Webb-Wood, S., Chow, A.Y., Ball, S.L., 2005. Neuroprotective effect of subretinal implants in the RCS rat. Investig. Ophthalmol. Vis. Sci. 46, 674–682.

Penn, R.D., Hagins, W.A., 1969. Signal transmission along retinal rods and the origin of the electroretinographic a-wave. Nature 223, 201–204.

Potts, A.M., Inoue, J., 1969. The electrically evoked response (EER) of the visual system. II. Effect of adaptation and retinitis pigmentosa. Investig. Ophthalmol. 8, 605–612.

Prusky, G.T., Alam, N.M., Beekman, S., Douglas, R.M., 2004. Rapid quantification of adult and developing mouse spatial vision using a virtual optomotor system. Investig. Ophthalmol. Vis. Sci. 45, 4611–4616.

Rahmani, S., Bogdanowicz, L., Thomas, J., Hetling, J.R., 2013. Chronic delivery of low-level exogenous current preserves retinal function in pigmented P23H rat. Vis. Res. 76, 105–113.

Robson, J.G., Frishman, L.J., 1995. Response linearity and kinetics of the cat retina: the bipolar cell component of the dark-adapted electroretinogram. Vis. Neurosci. 12, 837–850.

Robson, J.G., Frishman, L.J., 1998. Dissecting the dark-adapted electroretinogram. Doc. Ophthalmol. 95, 187–215.

Rozen, S., Skaletsky, H., 2000. Primer3 on the WWW for general users and for biologist programmers. Methods Mol. Biol. 132, 365–386.

Sabel, B.A., Fedorov, A.B., Naue, N., Borrmann, A., Herrmann, C., Gall, C., 2011. Non-invasive alternating current stimulation improves vision in optic neuropathy. Restor. Neurol. Neurosci. 29, 493–505.

Sato, T., Fujikado, T., Lee, T.S., Tano, Y., 2008a. Direct effect of electrical stimulation on induction of brain-derived neurotrophic factor from cultured retinal Muller cells. Investig. Ophthalmol. Vis. Sci. 49, 4641–4646.

Sato, T., Fujikado, T., Morimoto, T., Matsushita, K., Harada, T., Tano, Y., 2008b. Effect of electrical stimulation on IGF-1 transcription by L-type calcium channels in cultured retinal Muller cells. Jpn. J. Ophthalmol. 52, 217–223.

Sato, T., Lee, T.S., Takamatsu, F., Fujikado, T., 2008c. Induction of fibroblast growth factor-2 by electrical stimulation in cultured retinal Mueller cells. Neuroreport 19, 1617–1621.

Schatz, A., Arango-Gonzalez, B., Fischer, D., Enderle, H., Bolz, S., Rock, T., Naycheva, L., Grimm, C., Messias, A., Zrenner, E., Bartz-Schmidt, K.U., Willmann, G., Gekeler, F., 2012. Transcorneal electrical stimulation shows neuroprotective effects in retinas of light-exposed rats. Investig. Ophthalmol.

Vis. Sci. 53, 5552–5561.

Schatz, A., Rock, T., Naycheva, L., Willmann, G., Wilhelm, B., Peters, T., Bartz-Schmidt, K.U., Zrenner, E., Messias, A., Gekeler, F., 2011. Transcorneal electrical stimulation for patients with retinitis pigmentosa: a prospective, randomized, sham-controlled exploratory study. Investig. Ophthalmol. Vis. Sci. 52, 4485–4496.

Schmid, G., Neubauer, G., Mazal, P.R., 2003. Dielectric properties of human brain tissue measured less than 10 h postmortem at frequencies from 800 to 2450 MHz. Bioelectromagnetics 24, 423–430.

Schmid, H., Herrmann, T., Kohler, K., Stett, A., 2009. Neuroprotective effect of transretinal electrical stimulation on neurons in the inner nuclear layer of the degenerated retina. Brain Res. Bull. 79, 15–25.

Schmidt, S., Mante, A., Ronnefarth, M., Fleischmann, R., Gall, C., Brandt, S.A., 2013. Progressive enhancement of alpha activity and visual function in patients with optic neuropathy: a two-week repeated session alternating current stimulation study. Brain Stimul. 6, 87–93.

Sekirnjak, C., Jepson, L.H., Hottowy, P., Sher, A., Dabrowski, W., Litke, A.M., Chichilnisky, E.J., 2011. Changes in physiological properties of rat ganglion cells during retinal degeneration. J. Neurophysiol. 105, 2560–2571.

Sergeeva, E.G., Bola, M., Wagner, S., Lazik, S., Voigt, N., Mawrin, C., Gorkin, A.G., Waleszczyk, W.J., Sabel, B.A., Henrich-Noack, P., 2015. Repetitive transcorneal alternating current stimulation reduces brain idling state after long-term vision loss. Brain Stimul. 8, 1065–1073.

Sergeeva, E.G., Fedorov, A.B., Henrich-Noack, P., Sabel, B.A., 2012. Transcorneal alternating current stimulation induces EEG "aftereffects" only in rats with an intact visual system but not after severe optic nerve damage. J. Neurophysiol. 108, 2494–2500.

Shaked, I., Ben-Dror, I., Vardimon, L., 2002. Glutamine synthetase enhances the clearance of extracellular glutamate by the neural retina. J. Neurochem. 83, 574–580.

Sieving, P.A., Murayama, K., Naarendorp, F., 1994. Push-pull model of the primate photopic electroretinogram: a role for hyperpolarizing neurons in shaping the b-wave. Vis. Neurosci. 11, 519–532.

Stockton, R.A., Slaughter, M.M., 1989. B-wave of the electroretinogram. A reflection of ON bipolar cell activity. J. Gen. Physiol. 93, 101–122.

Stroh, C., Schulze-Osthoff, K., 1998. Death by a thousand cuts: an ever increasing list of caspase substrates. Cell Death Differ. 5, 997–1000.

Surowiec, A., Stuchly, S.S., Keaney, M., Swarup, A., 1986. In vivo and in vitro dielectric properties of feline tissues at low radiofrequencies. Phys. Med. Biol. 31, 901–909.

Turner, P.V., Albassam, M.A., 2005. Susceptibility of rats to corneal lesions after injectable anesthesia. Comp. Med. 55, 175–182.

Unoki, K., LaVail, M.M., 1994. Protection of the rat retina from ischemic injury by brain-derived neurotrophic factor, ciliary neurotrophic factor, and basic fibroblast growth factor. Investig. Ophthalmol. Vis. Sci. 35, 907–915.

Utz, P.J., Anderson, P., 2000. Life and death decisions: regulation of apoptosis by proteolysis of signaling molecules. Cell Death Differ. 7, 589–602.

Villegas-Perez, M.P., Vidal-Sanz, M., Lund, R.D., 1996. Mechanism of retinal ganglion cell loss in inherited retinal dystrophy. Neuroreport 7, 1995–1999.

Wang, X., Mo, X., Li, D., Wang, Y., Fang, Y., Rong, X., Miao, H., Shou, T., 2011. Neuroprotective effect of transcorneal electrical stimulation on ischemic damage in the rat retina. Exp. Eye Res. 93, 753–760.

Wenzel, A., Grimm, C., Samardzija, M., Remé, C.E., 2005. Molecular mechanisms of light-induced photoreceptor apoptosis and neuroprotection for retinal degeneration. Prog. Retin Eye Res. 24, 275–306.

Willmann, G., Schaferhoff, K., Fischer, M.D., Arango-Gonzalez, B., Bolz, S., Naycheva, L., Rock, T., Bonin, M., Bartz-Schmidt, K.U., Zrenner, E., Schatz, A., Gekeler, F., 2011. Gene expression profiling of the retina after transcorneal electrical stimulation in wild-type Brown Norway rats. Investig. Ophthalmol. Vis. Sci. 52, 7529–7537.

Wrobel, W.G., Banzhaf, A., Blaess, G., Eipper, C., Harscher, A., Hekmat, A., Moller, A., Mohrlok, R., Patzold, J., 2011. A new system for the treatment of retinal degeneration. Biomed. Tech. Berl. 56, 277–282.

Yang, J.Y., Michod, D., Walicki, J., Murphy, B.M., Kasibhatla, S., Martin, S.J., Widmann, C., 2004. Partial cleavage of RasGAP by caspases is required for cell survival in mild stress conditions. Mol. Cell Biol. 24, 10425–10436.

Yu, D.-Y., Cringle, S., Valter, K., Walsh, N., Lee, D., Stone, J., 2004. Photoreceptor death, trophic factor expression, retinal oxygen status, and photoreceptor function in the P23H rat. Investig. Ophthalmol. Vis. Sci. 45, 2013–2019.

Yu, X.H., Zhang, H., Wang, Y.H., Liu, L.J., Teng, Y., Liu, P., 2009. Time-dependent reduction of glutamine synthetase in retina of diabetic rats. Exp. Eye Res. 89, 967–971.

Zhang, Y., Yao, G., Gao, Y., Hofeldt, K.J., Lei, B., 2007. Frequency spectrum and amplitude analysis of dark- and light-adapted oscillatory potentials in albino mouse, rat, and rabbit. Doc. Ophthalmol. 115, 85–93.

Zhou, W.T., Ni, Y.Q., Jin, Z.B., Zhang, M., Wu, J.H., Zhu, Y., Xu, G.Z., Gan, D.K., 2012. Electrical stimulation ameliorates light-induced photoreceptor degeneration in vitro via suppressing the proinflammatory effect of microglia and enhancing the neurotrophic potential of Muller cells. Exp. Neurol. 238, 192–208.